Supporting Information

Effect of Interfacial Recombination, Bulk Recombination and Carrier Mobility on J-V Hysteresis Behaviors of Perovskite Solar Cells: A Drift-Diffusion Simulation Study

Jin Xiang,[†, ‡, ǀ] Yana Li,[†, ǀ] Feng Huang,[§, ǀ] and Dingyong Zhong*, [†, ǀ]

[†]School of Physics, Sun Yat-sen University, Xingang Xi Road 135, 510275 Guangzhou, China

[‡]School of Materials Science and Engineering, Sun Yat-sen University, Xingang Xi Road 135, 510275 Guangzhou, China

[§]School of Materials, Sun Yat-sen University, Xingang Xi Road 135, 510275 Guangzhou, China

[ǀ]State Key Laboratory of Optoelectronic Materials and Technologies, Sun Yat-sen University, Xingang Xi Road 135, 510275 Guangzhou, China

Corresponding Author

*E-mail address: dyzhong@mail.sysu.edu.cn.

Methodology

The COMSOL software is used to perform the *J*-*V* characteristic simulation. For devices with only interfacial recombination, a radiative recombination coefficient ($B_{radiative}$) of 2×10^{-11} $cm^3\cdot s^{-1}$ is first added in perovskite active layer and then the Shockley-Read-Hall (SRH) recombination mechanism is added in interfacial recombination layers (S) to mimic interfacial recombination process. This SRH recombination lifetime is marked as $\tau_{interface}$ (interfacial recombination lifetime). For devices with only bulk recombination, a $B_{radiative}$ of 2×10^{-11} $cm^3\cdot s^{-1}$ is first added in perovskite active layer and then the SRH recombination mechanism is added in perovskite active layer, too. This SRH recombination lifetime is marked as τ_{bulk} (bulk recombination lifetime).

In the simulation, the devices are first held at a forward bias voltage of 1.2 V (or 1.35 V, in cases with $V_{OC} > 1.2$ V) for 100 s to allow ions to migrate and achieve an equilibrium condition. Next, bias voltage is scanned from 1.2 V (or 1.35 V) to −0.2 V (reverse scan), and immediately scanned back to 1.2 V (or 1.35 V) (forward scan) to obtain a complete *J*-*V* loop. The duration time for each *J*-*V* loop is fixed at 0.1 s (scan rate = 28 $V\cdot s^{-1}$), 8.1 s (scan rate = 350 $mV\cdot s^{-1}$), 20.1 s (scan rate = 140 $mV\cdot s^{-1}$), 40.1 s (scan rate = 70 $mV\cdot s^{-1}$) and 100.1 s (scan rate = 28 $mV\cdot s^{-1}$) to mimic fast and slow scanning protocols (scan rate = voltage range/duration time). Figure S1 shows the scanning protocol of the simulation. The voltage step is 20 mV. And at the end of each voltage step, the voltage value and current density value are recorded to produce *J*-*V* curves (indicated by the red arrows).

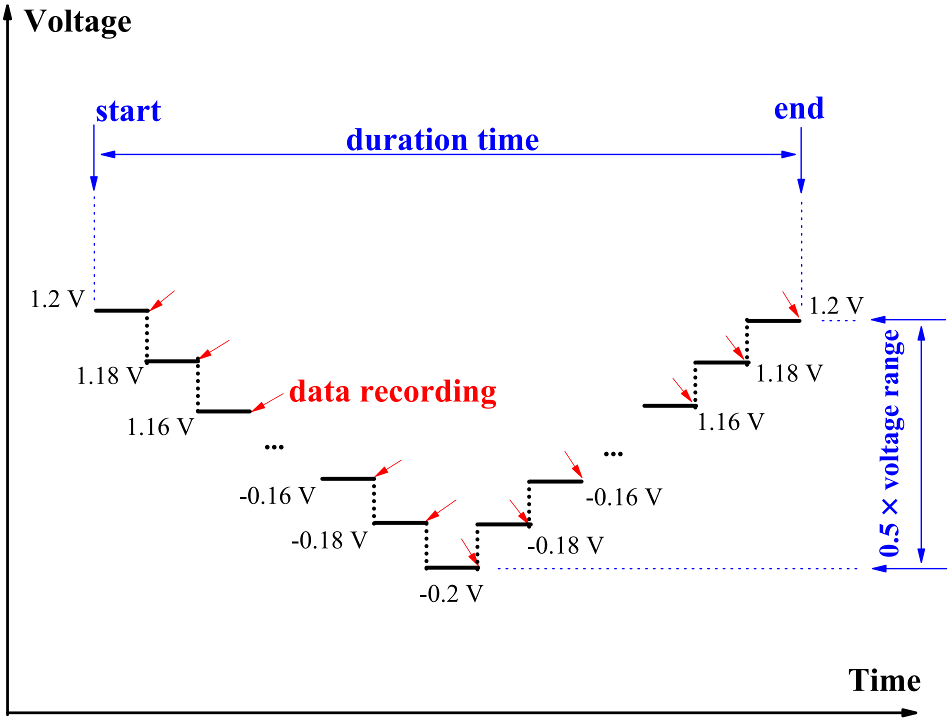

Figure S1. Scanning protocol in our simulation.

Controlling equations

Poinsson's equation and drift-diffusion equations of charge carriers and ions are shown as follow

$$\frac{\partial n}{\partial t} = \frac{1}{q}\frac{\partial J_n}{\partial x} - R + G, \quad J_n = q\mu_n nE + qD_n\frac{\partial n}{\partial x}$$

$$\frac{\partial p}{\partial t} = -\frac{1}{q}\frac{\partial J_p}{\partial x} - R + G, \quad J_p = q\mu_{\mathrm{p}} pE - qD_p\frac{\partial p}{\partial x}$$

$$\frac{\partial N}{\partial t} = \frac{1}{q}\frac{\partial J_N}{\partial x}, \quad J_N = q\mu_N NE + qD_N\frac{\partial N}{\partial x}$$

$$\frac{\partial P}{\partial t} = -\frac{1}{q}\frac{\partial J_P}{\partial x}, \quad J_P = q\mu_P PE - qD_P\frac{\partial P}{\partial x}$$

$$\frac{d^2\varphi}{dx^2} = \frac{q(n + N + Nd^- - p - P - Nd^+)}{\varepsilon_0\varepsilon_r}$$

where *n, p, N, P* are electron, hole, anion and cation density. $\mu_{n,p,N,P}$ and $D_{n,p,N,P} = \frac{k_B T}{q} \mu_{n,p,N,P}$ are their drift mobility and diffusion coefficient, respectively. φ and $E = \frac{d\varphi}{dx}$ are electric potential and electric field. ε_0, ε_r, q, k_B, T are vacuum permittivity, relative permittivity, elementary charge, Boltzmann constant and absolute temperature. Nd^- and Nd^+ are p-type and n-type doping concentration. The mobile ions are assumed to be the same concentration of $N = P = 5\times10^{23}$ m^{-3}, and ions are added only in perovskite active layer. At perovskite boundaries, no ions can move out ($J_N = J_P = 0$). For electrons and holes, the continuous quasi fermi level boundary condition is adopted at all boundaries. $G = G_{light}$ is the generation rate for electrons (holes). A uniform generation rate of $G_{light} = 3.3\times10^{27}$ m^{-3}·s^{-1} is adopted in perovskite active layer, yielding a short circuit current density of 21.15 mA·cm^{-2}. $R = R_{radiative} + R_{SRH}$ is the recombination rate for electrons (holes). The radiative recombination rate is

$$R_{radiative} = B_{radiative}(np - n_i p_i)$$

where $B_{radiative}$ is radiative recombination coefficient. n_i and p_i are intrinsic carrier density. The SRH recombination rate is

$$R_{SRH} = \frac{np - n_i p_i}{\tau_n p + \tau_p n}$$

$$\tau_{n,p} = \frac{1}{N_t v_{th} \sigma_{n,p}}$$

where N_t, v_{th}, $\sigma_{n,p}$ and $\tau_{n,p}$ are trap density, electron (hole) thermal velocity, electron (hole) capture cross-section and electron (hole) lifetime. Here, a reduced form of SRH recombination is adopted, in which N_t, v_{th}, and $\sigma_{n,p}$ are compress into $\tau_{n,p}$. Thus, the trap density (N_t) is not considered in the Poinsson's Equation. The trap energy level is set in the middle of the bandgap. For all case, we assume that $\tau_n = \tau_p$. In perovskite bulk, the SRH recombination lifetime is marked as τ_{bulk} (bulk recombination lifetime). In interfacial recombination layers, the SRH recombination life time is marked as $\tau_{interface}$ (interfacial recombination lifetime).

Conversion of interfacial recombination lifetime ($\tau_{interface}$) to surface recombination velocity ($V_{surface}$)

At TiO_2/perovskite interface, the $\tau_{interface}$ in this interfacial recombination layer is assumed to be 20, 1, 0.2, 0.05 ns. Since TiO_2 layer is n-type doped and perovskite layer is an intrinsic semiconductor, thus, in this interfacial recombination layer, $n >> p$. And we ignore the intrinsic carrier density term. The SRH recombination rate is reduce to

$$R_{SRH} = \frac{p}{\tau_p}$$

where the unit of R_{SRH} is $m^{-3}\cdot s^{-1}$. The thickness of this interfacial recombination layer is d = 0.01 nm. And we assume that hole density is uniformly distributed within interfacial recombination layer, thus the surface recombination rate is

$$R_{surface} = \int_0^d R_{SRH} dx = \int_0^d \frac{p}{\tau_p} dx = d \frac{1}{\tau_p} p = V_{surface} p$$

where $V_{surface} = d \frac{1}{\tau_p}$ is the surface recombination velocity. For d = 0.01 nm and $\tau_{interface}$ = 20, 1, 0.2, 0.05 ns, surface recombination velocity is $V_{surface}$ = 0.05, 1, 5, 20 $cm\cdot s^{-1}$. Noted that this value is slightly smaller than reported (reference 2). In interfacial recombination layer, the effective density of state in conduction (N_C) and valance (N_V) band is 1×10^{26} m^{-3}, 20 times higher than that of perovskite layer (5×10^{24} m^{-3}). If N_C (N_V) is set as 5×10^{24} m^{-3} in interfacial recombination layer, in order to obtain the same open circuit voltage, $\tau_{interface}$ should be 20 times smaller (1, 0.05, 0.01, 0.0025 ns), Thus surface recombination velocity should be $V_{surface}$ = 1, 20, 100, 400 cm·s^{-1}. Now, this value is in accordance with literature report (reference 2).

$\tau_{interface}$ (ns)	J_{SC} ($mA\cdot cm^{-2}$) _no ions	PCE (%) _no ions	FF _no ions	V_{OC} (V) _no ions
$R_{radiative}$	**21.15**	**24.3**	**0.884**	**1.3**
20	**21.15**	**21.49**	**0.825**	**1.216**
1	**21.15**	**19.6**	**0.845**	**1.097**
0.2	**21.15**	**18.42**	**0.828**	**1.052**
0.05	**21.15**	**17.25**	**0.803**	**1.016**

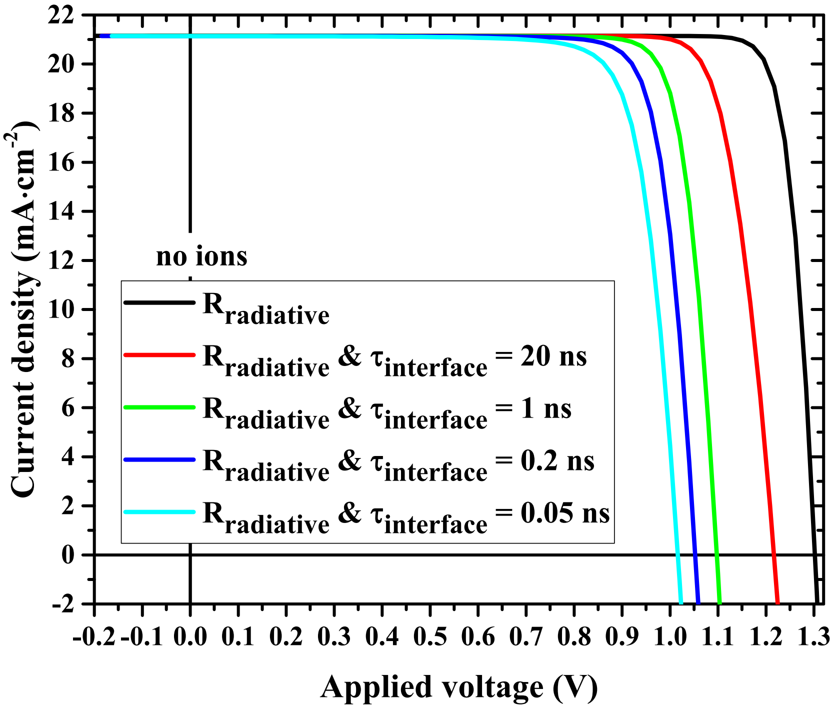

Figure S2. Simulated *J-V* hysteresis loops of devices with only interfacial recombination. The black line shows the room temperature radiative limit for PVSCs with band gap of 1.6 eV, by accounting for $B_{radiative} = 2\times10^{-11}$ $cm^3\cdot s^{-1}$. The red, green, blue, and light-blue lines are *J-V* curves by additionally accounting for different values of $\tau_{interface}$: 20 ns, 1 ns, 0.2 ns and 0.05 ns, respectively, without mobile ions. The device parameters for these curves are summarized in the above table.

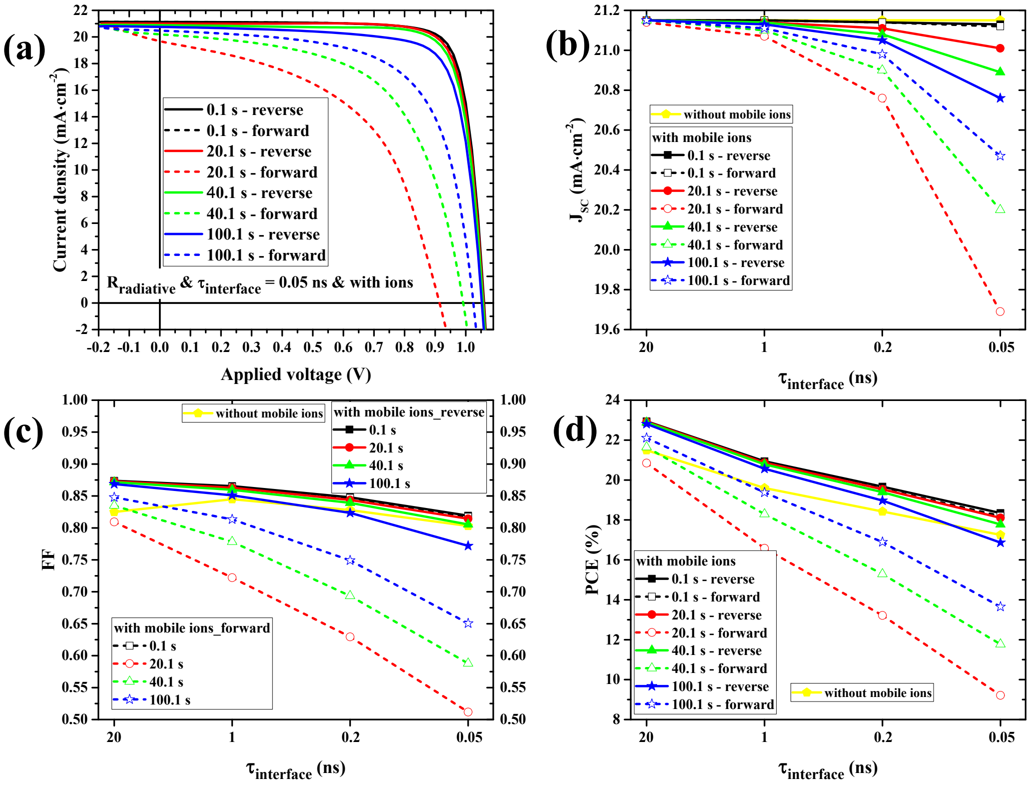

Figure S3. Simulated *J-V* hysteresis loops of devices with only interfacial recombination. $B_{radiative} = 2\times10^{-11}$ $cm^3\cdot s^{-1}$ is first added in perovskite active layer. Then, the black (duration time = 0.1 s), red (duration time = 20.1 s), green (duration time = 40.1 s) and blue (duration time = 100.1 s) loops are *J-V* curves by additionally accounting for different values of $\tau_{interface}$: 20 ns, 1 ns, 0.2 ns and 0.05 ns, with mobile ions. (a) *J-V* hysteresis loops with $\tau_{interface}$: = 0.05 ns. (b-d) Summarized J_{SC} , FF and PCE for each *J-V* curves. Yellow line represents the devices without mobile ions. For all cases, line (dash line) represent reverse (forward) scan.

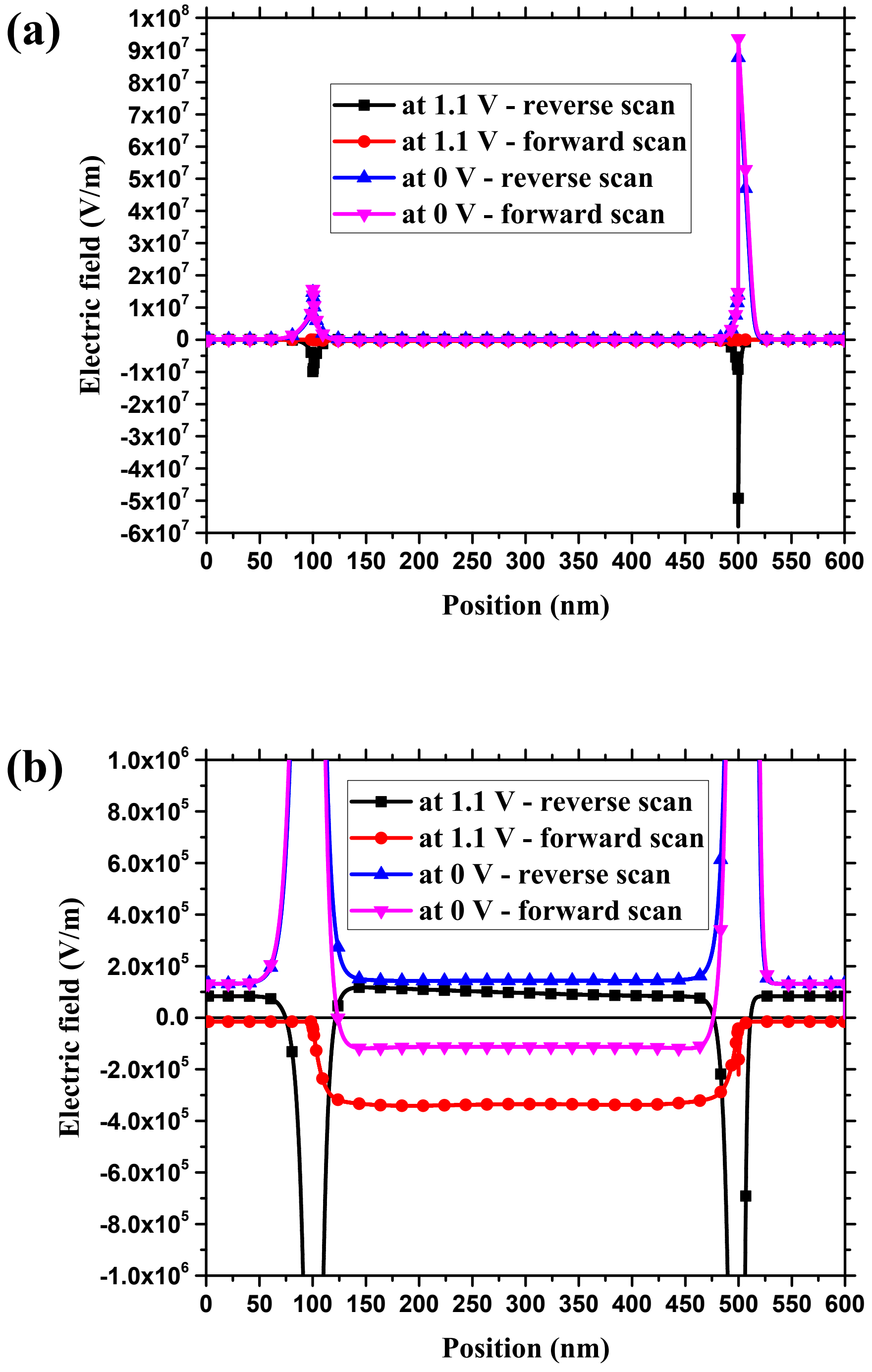

Figure S4. Spatial distribution of electric field in the device with only interfacial recombination ($\tau_{\mathrm{interface}}$ = 1 ns, duration time = 20.1 s). At voltage bias of 1.1 V and 0 V.

τ_{bulk} (ns)	J_{SC} ($mA\cdot cm^{-2}$) _no ions	PCE (%) _no ions	FF _no ions	V_{OC} (V) _no ions
$R_{radiative}$	21.15	24.3	0.884	1.3
500	21.15	21.04	0.802	1.24
200	21.13	19.64	0.771	1.205
50	21.08	17.44	0.723	1.144
10	20.8	14.6	0.669	1.048

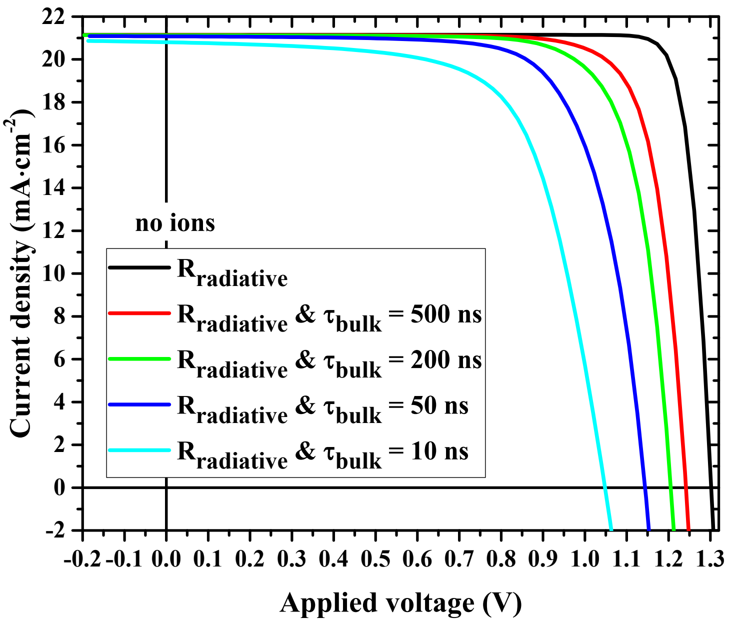

Figure S5. Simulated *J-V* hysteresis loops of devices with only bulk recombination. The black line shows the room temperature radiative limit for PVSCs with band gap of 1.6 eV, by accounting for $B_{radiative}$ = 2×10^{-11} $cm^3\cdot s^{-1}$. The red, green, blue, and light-blue lines are *J-V* curves by additionally accounting for different values of τ_{bulk}: 500 ns, 200 ns, 50 ns and 10 ns, respectively, without mobile ions. The device parameters for these curves are summarized in the above table.

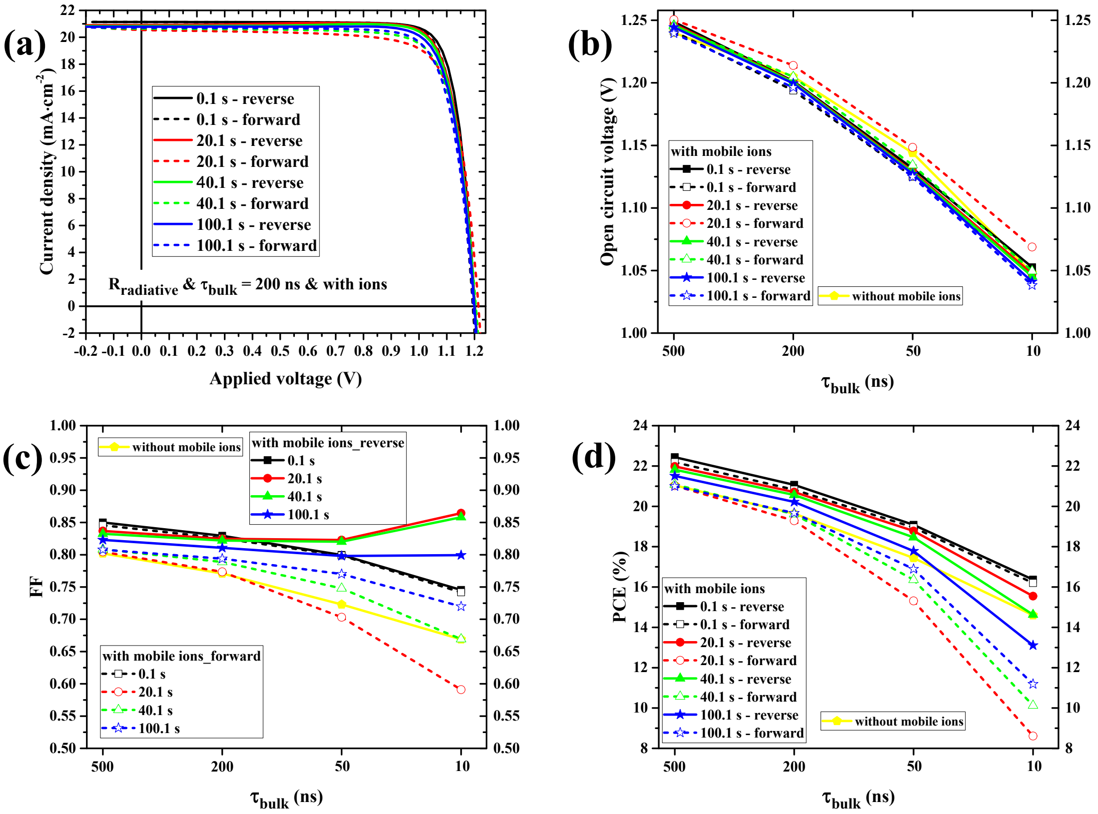

Figure S6. Simulated *J-V* hysteresis loops of devices with only bulk recombination. $B_{radiative} = 2\times10^{-11}$ cm^3·s^{-1} is first added in perovskite active layer. Then, the black (duration time = 0.1 s), red (duration time = 20.1 s), green (duration time = 40.1 s) and blue (duration time = 100.1 s) loops are *J-V* curves by additionally accounting for different values of τ_{bulk}: 500 ns, 200 ns, 50 ns and 10 ns, with mobile ions. (a) *J-V* hysteresis loops with τ_{bulk}: = 200 ns. (b-d) Summarized V_{OC} , FF and PCE for each *J-V* curves. Yellow line represents the devices without mobile ions. For all cases, line (dash line) represent reverse (forward) scan.

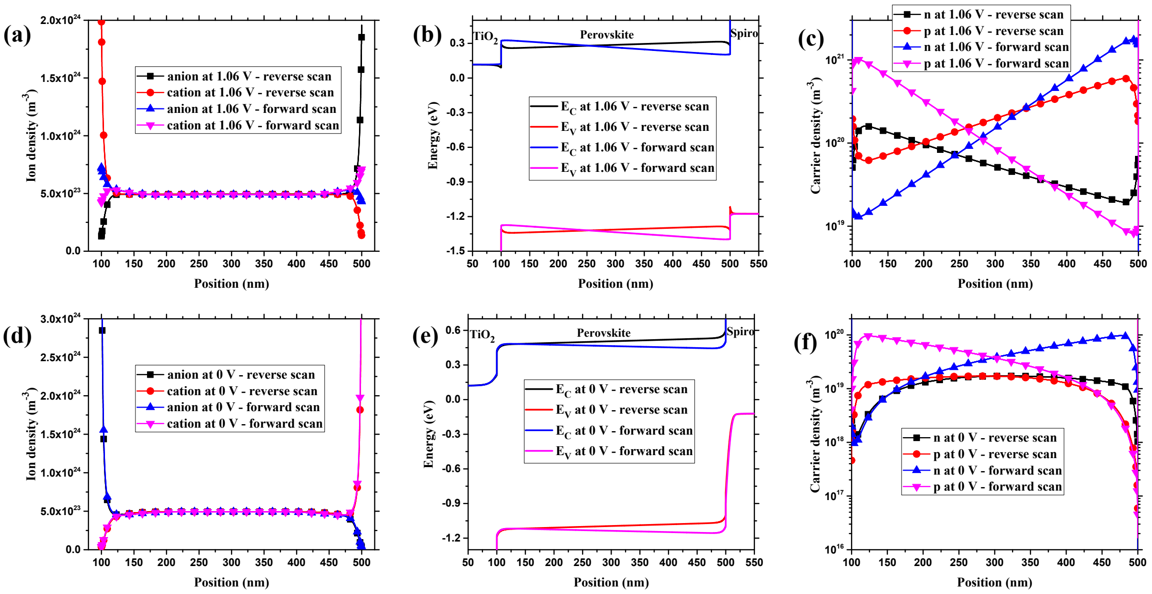

Figure S7. Spatial distribution of ion density, energy level and carrier density in the device with only bulk recombination (τ_{bulk} = 10 ns, duration time = 20.1 s). (a) to (c) At voltage bias of 1.06 V. (d) to (f) At zero voltage bias.

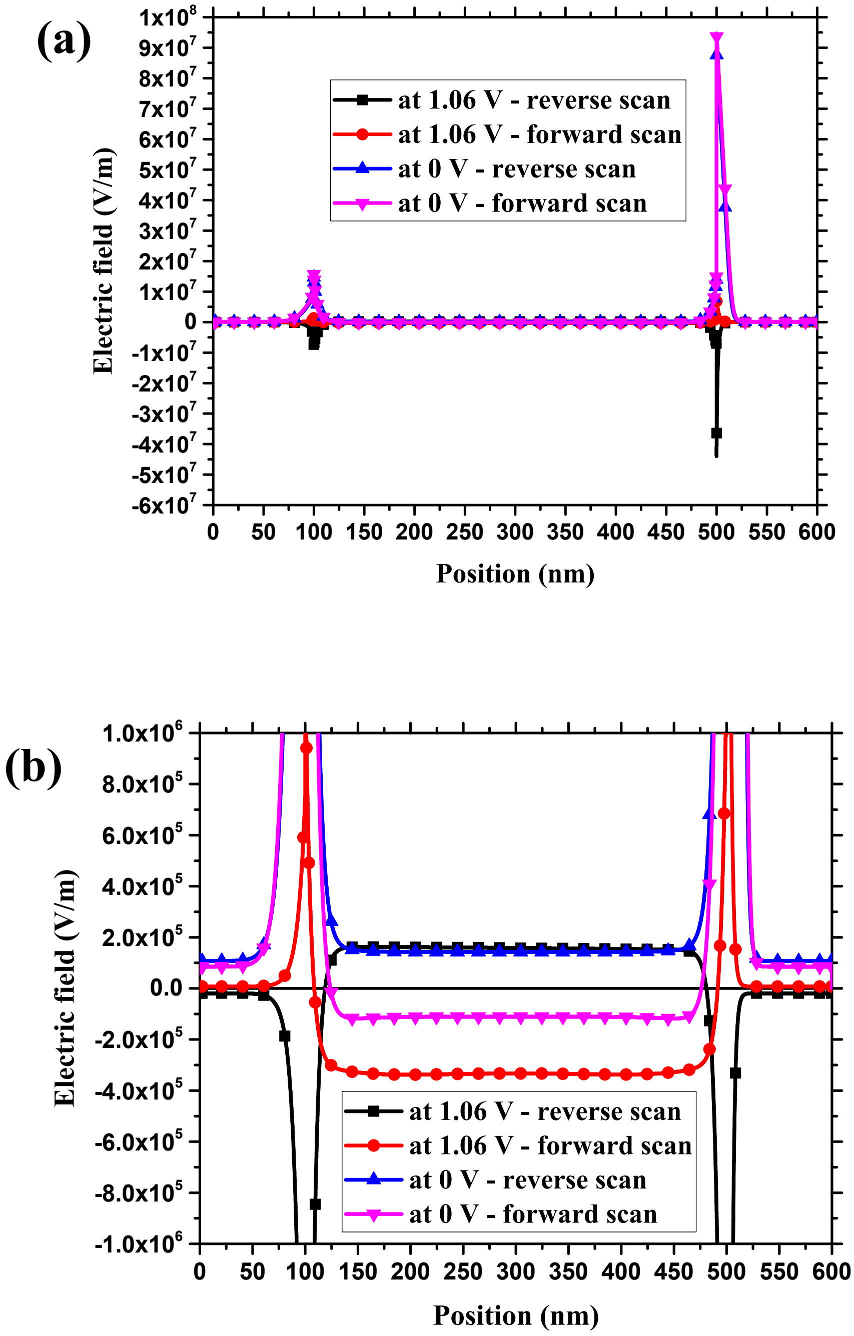

Figure S8. Spatial distribution of electric field in the device with only bulk recombination (τ_{bulk} = 10 ns, duration time = 20.1 s). At voltage bias of 1.06 V and 0 V.

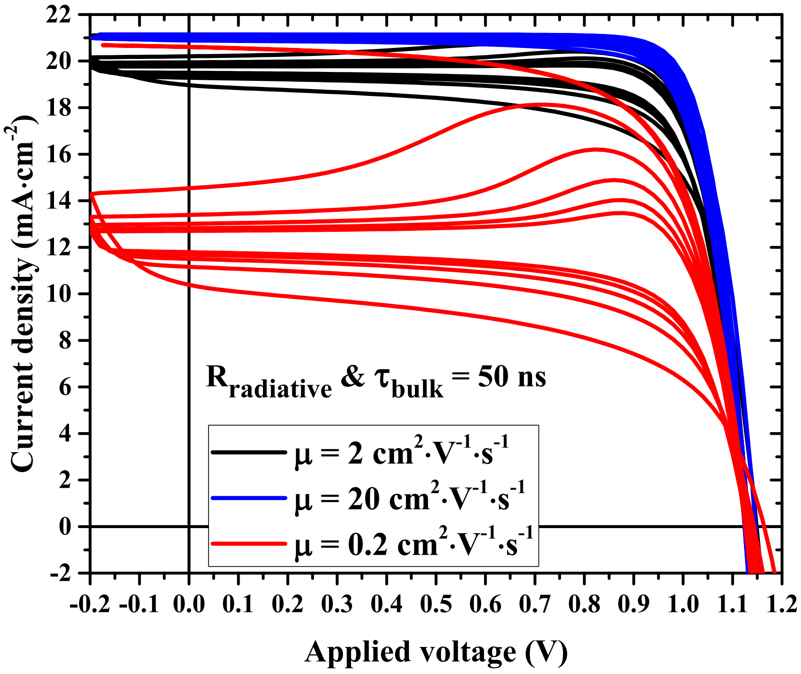

Figure S9. *J*-*V* hysteresis loops with only bulk recombination (τ_{bulk} = 50 ns). Consideration of different carrier mobility μ in the devices. This is the same as that in figure 7a-c, but drawn in one figure.

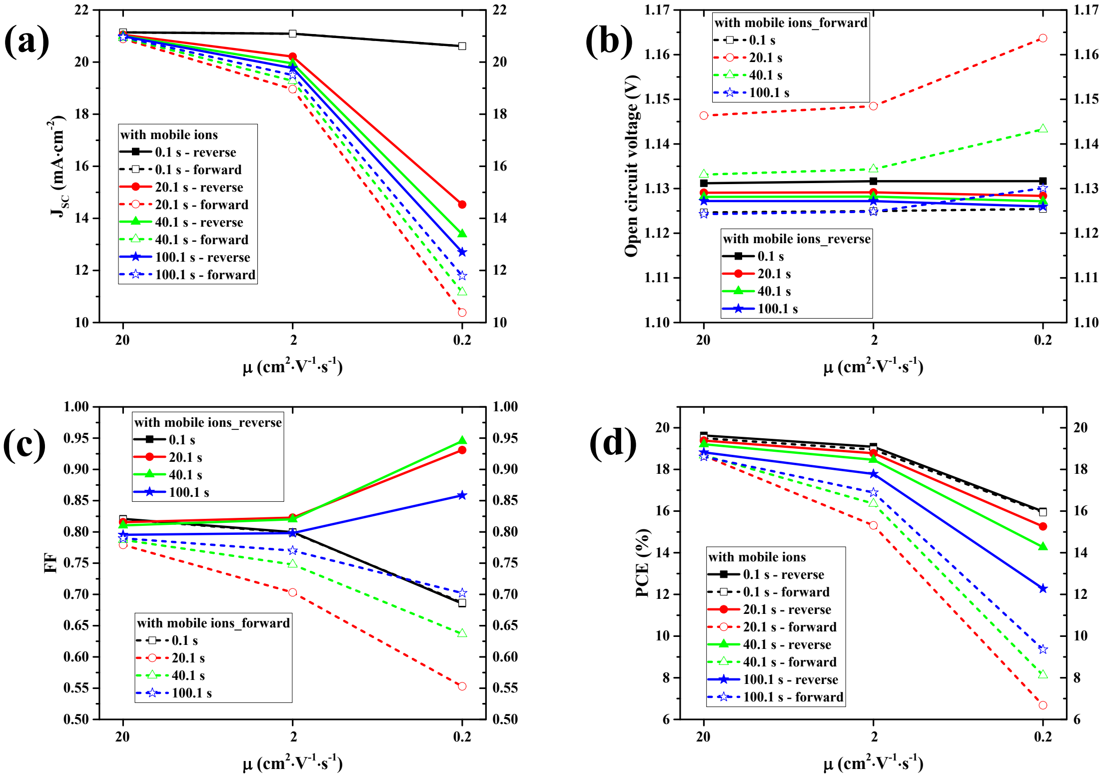

Figure S10. Summarized J_{SC}, V_{OC}, FF and PCE for each *J-V* curves shown in figure 7a-c. The black (duration time = 0.1 s), red (duration time = 20.1 s), green (duration time = 40.1 s) and blue (duration time = 100.1 s) lines are taken from *J-V* curves with different scan rate, with mobile ions. For all cases, line (dash line) represent reverse (forward) scan.

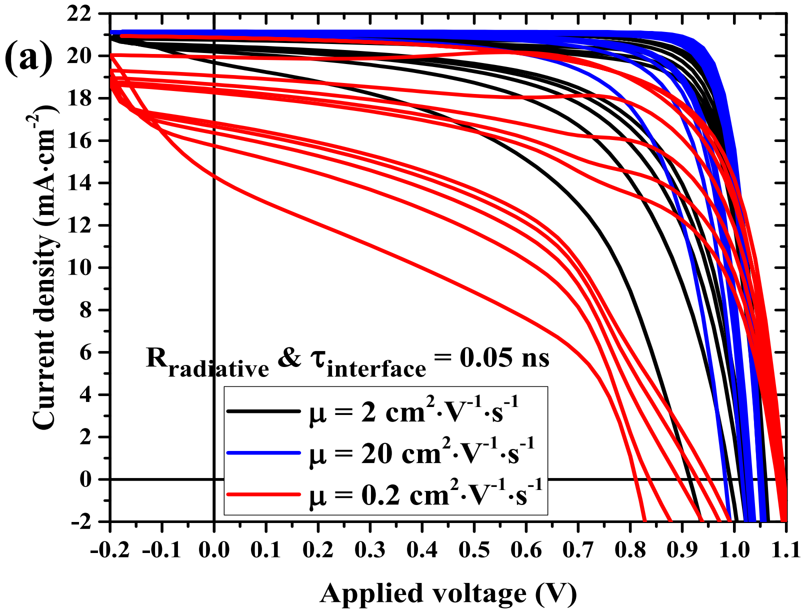

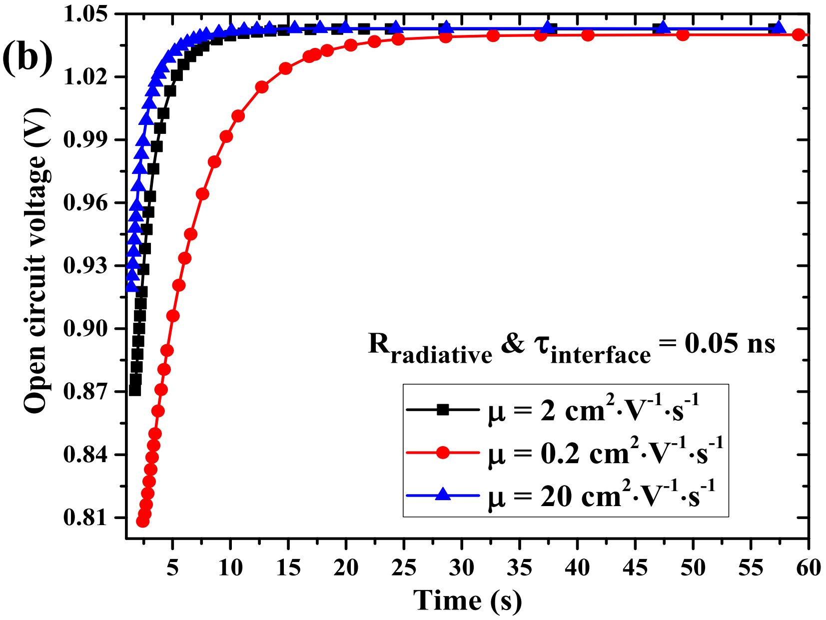

Figure S11. (a) *J*-*V* hysteresis loops with only interfacial recombination ($\tau_{\text{interface}}$ = 0.05 ns). Consideration of different carrier mobility μ in the devices. This is the same as that in figure 7d-f, but drawn in one figure. (b) The corresponding V_{OC}-t dynamics for devices in (a).

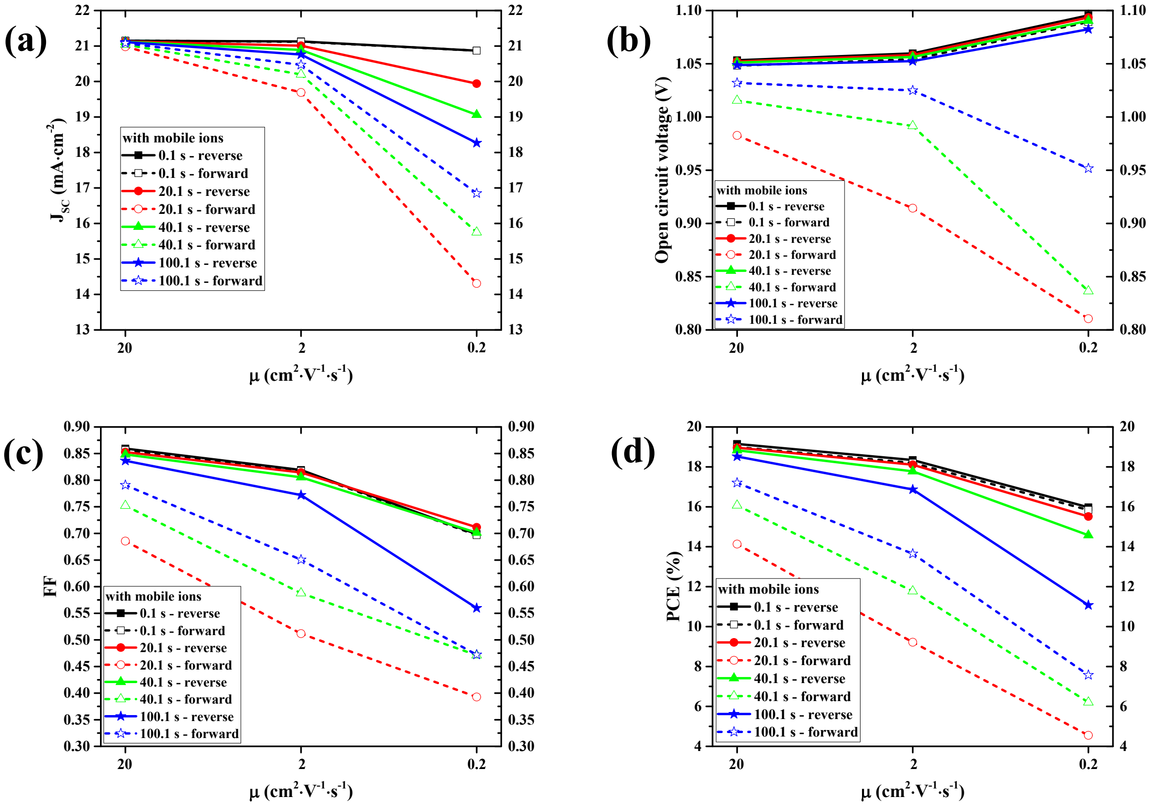

Figure S12. Summarized J_{SC}, V_{OC}, FF and PCE for each *J*-*V* curves shown in figure 7d-f. The black (duration time = 0.1 s), red (duration time = 20.1 s), green (duration time = 40.1 s) and blue (duration time = 100.1 s) lines are taken from *J*-*V* curves with different scan rate, with mobile ions. For all cases, line (dash line) represent reverse (forward) scan.

Other considerations:

Here, in our work, we choose these parameters (Table 1) to represent a typical FTO/TiO_2/$CH_3NH_3PbI_3$/Spiro-OMeTAD/Au solar cell. But, as reviewer have mentioned, some parameters may affect the simulation results.

1. The mobility of CTLs. Here, we increase the mobility of CTLs from 1×10^{-4} $cm^2\cdot V^{-1}\cdot s^{-1}$ to 1 $cm^2\cdot V^{-1}\cdot s^{-1}$. The resulting *J-V* curves are shown below in Figure S13.

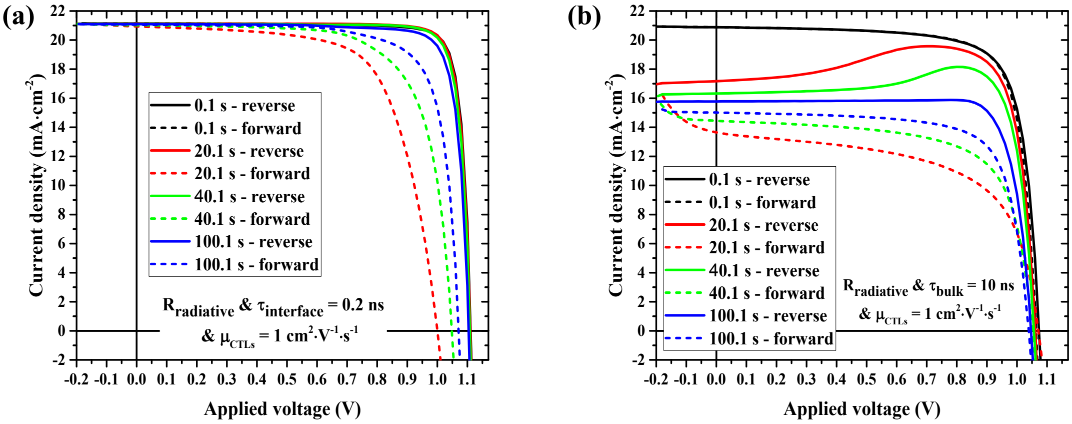

Figure S13. Simulated *J-V* hysteresis loops with, (a) only interfacial recombination ($\tau_{interface}$ = 0.2 ns.), (b) only bulk recombination (τ_{bulk} = 10 ns). The mobility of CTLs is 1 $cm^2\cdot V^{-1}\cdot s^{-1}$.

2. The relative permittivity of ETL. Here, in order to mimic a perovskite solar cell with organic ETL, we change the relative permittivity of TiO_2 layer from 31 to 3. The resulting *J-V* curves are shown below in Figure S14.

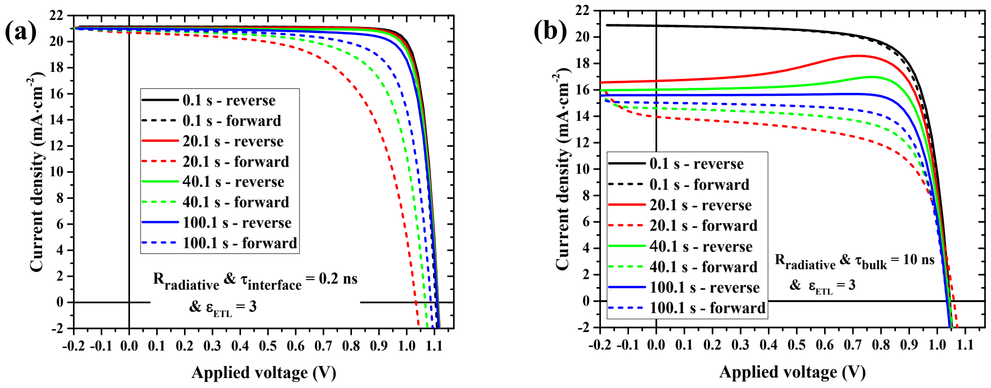

Figure S14. Simulated *J-V* hysteresis loops with, (a) only interfacial recombination ($\tau_{interface}$ = 0.2 ns.), (b) only bulk recombination (τ_{bulk} = 10 ns). The relative permittivity of TiO_2 layer is 3.

3. The doping concentration of perovskite layer. In our work, the perovskite layer is intrinsic. Here, the perovskite layer is n-type doped with a doping concentration of 10^{22} m^{-3} (Since $n = N_d = N_C \exp(\frac{E_C - E_F}{k_B T}), \Rightarrow E_C - E_F = 0.16\ \mathrm{eV}$. As for the doping level of perovskite layer, please refer to “DOI: 10.1063/1.4899051” for more information.). The resulting *J-V* curves are shown below in Figure S15. The doping of perovskite layer should modulate the electric field distribution of the solar cell, thus resulting in different hysteresis behaviors. But, the simulated *J-V* hysteresis loops are almost unchanged. Qualitatively, mobile ions will screen the built-in electric field within a solar cell, result in almost the same electric field distribution.

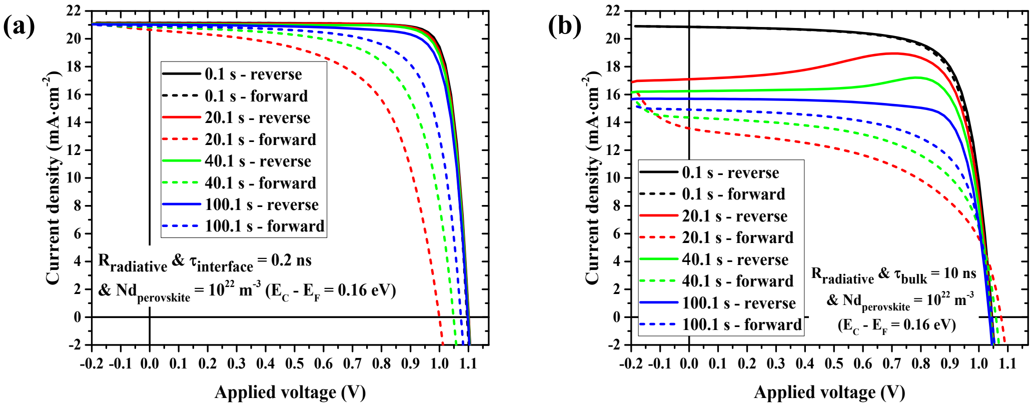

Figure S15. Simulated *J-V* hysteresis loops with, (a) only interfacial recombination ($\tau_{interface}$ = 0.2 ns.), (b) only bulk recombination (τ_{bulk} = 10 ns). The perovskite layer is n-type doped with a doping concentration of 10^{22} m^{-3}.

4. The built-in potential. In our work, a built-in potential of ~1 V (Page 6 in the main text) is adopted in the simulation. Here, we increase the doping concentration of CTLs from 10^{24} m^{-3} to 10^{26} m^{-3}, yielding a built-in potential of 1.2 V. The resulting *J-V* curves are shown below in Figure S16.

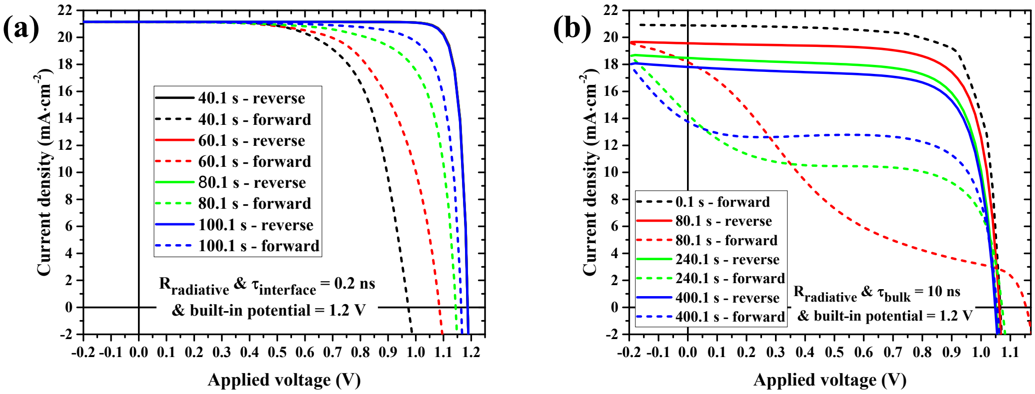

Figure S16. Simulated *J-V* hysteresis loops with, (a) only interfacial recombination ($\tau_{interface}$ = 0.2 ns.), (b) only bulk recombination (τ_{bulk} = 10 ns). The built-in potential is 1.2 V.

5. Energy level alignment at perovskite/CTLs interfaces. In our work, the E_C and E_V of perovskite layer is 3.95 and 5.55 eV. And at perovskite/CTLs interfaces, the conduction band offset at perovskte/ETL interface is equal to the valance band offset at perovskite/HTL interface (ΔE_C=ΔE_V=0.2 eV). Here, we change the E_C of ETL layer to 3.95 eV, resulting in a ΔE_C=0 eV (at perovskte/ETL interface) and ΔE_V=0.2 eV (at perovskte/HTL interface). The resulting *J-V* curves are shown below in Figure S17. Noted that, in Fig. S17a, we get an inverted hysteresis phenomenon (reverse scan gives smaller V_{OC} and larger J_{SC} than forward scan does).

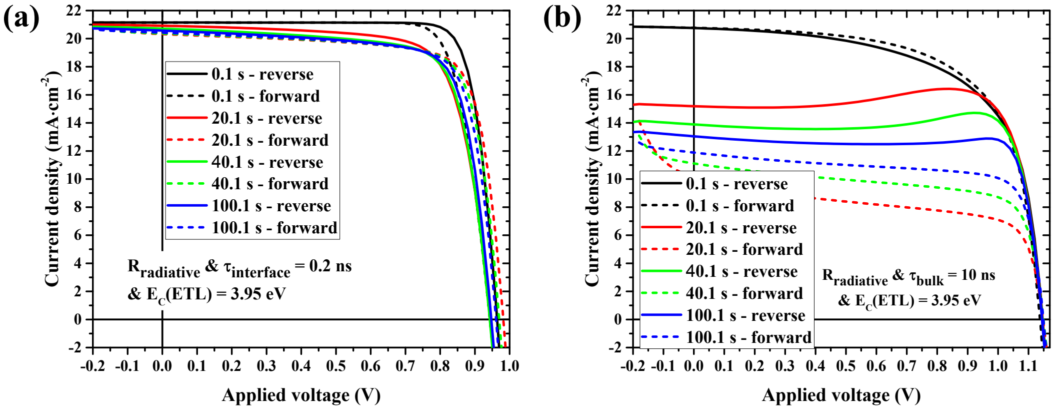

Figure S17. Simulated *J-V* hysteresis loops with, (a) only interfacial recombination ($\tau_{interface}$ = 0.2 ns.), (b) only bulk recombination (τ_{bulk} = 10 ns). The E_C of ETL layer is changed to 3.95 eV.

In a word, we believe that, in most cases, our conclusion still holds.

References

[S1]. Sze, S. M. Physics of Semiconductor Devices; Wiley: New York, **1981**.

[S2]. Liu, Z.; Krückemeier, L.; Krogmeier, B.; Klingebiel, B.; Márquez, J. A.; Levcenko, S.; Öz, S.; Mathur, S.; Rau, U.; Unold, T.; Kirchartz, T., Open-Circuit Voltages Exceeding 1.26 V in Planar Methylammonium Lead Iodide Perovskite Solar Cells. *ACS Energy Lett.* **2019**, *4*, 110-117.